Study of the lowlying states of Ge2 and Ge− 2 using negative ion zero electron kinetic energy spectroscopy

Caroline C. Arnold, Cangshan Xu, Gordon R. Burton, and Daniel M. Neumark

Citation: The Journal of Chemical Physics **102**, 6982 (1995); doi: 10.1063/1.469091
View online: http://dx.doi.org/10.1063/1.469091
View Table of Contents: http://scitation.aip.org/content/aip/journal/jcp/102/18?ver=pdfcov
Published by the AIP Publishing

Study of the low-lying states of Ge_2 and Ge_2^- using negative ion zero electron kinetic energy spectroscopy

Caroline C. Arnold,[a] Cangshan Xu, Gordon R. Burton,[b] and Daniel M. Neumark[c]
Department of Chemistry, University of California, Berkeley, California 94720, and Chemical Sciences Division, Lawrence Berkeley Laboratories, Berkeley, California 94720

(Received 16 December 1994; accepted 2 February 1995)

The low-lying states of Ge_2 and Ge_2^- are probed using negative ion zero electron kinetic energy (ZEKE) spectroscopy. The ZEKE spectrum of Ge_2^- yields an electron affinity of 2.035 ± 0.001 eV for Ge_2, as well as term energies and vibrational frequencies for the low-lying states of Ge_2^- and Ge_2. Specifically, we observe transitions originating from the anion $^2\Pi_u(3/2)$ ground state and $^3\Sigma_g^+$ excited state ($T_e = 279 \pm 10$ cm^{-1}) to several triplet and singlet states of Ge_2. Term values and vibrational frequencies are determined for the Ge_2 $^3\Sigma_g^+$ ground state, the low-lying $^3\Pi_u$ excited state ($T_e = 337$ cm^{-1} for the 2_u spin–orbit component), and the somewhat higher lying $^1\Delta_g$, $^3\Sigma_g^+$, and $^1\Pi_u$ states. We also determine the zero-field splitting for the $X0_g^+$ and 1_g components of the $^3\Sigma_g^+$ state and the splittings between the 2_u, 1_u, and $0_u^\pm$ spin–orbit components of the $^3\Pi_u$ state. Detailed comparisons are made with Si_2 and Si_2^-. © *1995 American Institute of Physics.*

I. INTRODUCTION

The ongoing effort to characterize the geometries and electronic structures of small elemental semiconductor clusters has been fueled by theoretical studies for at least 10 years. However, experiments on these elusive species have proven extremely difficult, primarily due to the lack of mass specificity of most cluster sources. Thus, for example, while Si_2 has been studied in a series of *ab initio* calculations dating back to 1980,[1] the experimental characterization of its low-lying electronic states has been accomplished only recently using negative ion photodetachment techniques.[2] While matrix isolation spectroscopy has been used with some success to obtain vibrationally resolved spectra of silicon, germanium, or mixed semiconductor clusters (primarily dimers),[3,4] most spectroscopic information at the vibrationally resolved level on larger clusters has come from intrinsically mass-selective techniques such as negative ion photodetachment[5,6] or matrix deposition of mass-selected clusters.[7]

As an extension of our previous work on Si_2^-, this paper presents the zero electron kinetic energy, or ZEKE spectrum of Ge_2^-. A comparison of this spectrum with the lower resolution photoelectron spectrum (PES) of Ge_2^- recently obtained in our laboratory[8] and the matrix spectroscopy work on Ge_2 by Li, Van Zee, and Weltner[3] enables us to map out the five lowest-lying states of Ge_2 and the two low-lying states of Ge_2^-; these are shown schematically in Fig. 1. The germanium dimer has been predicted to be electronically very similar to silicon dimer, with a $^3\Sigma_g^-$ $(\cdots 2\sigma_g^2 1\pi_u^2)$ ground state and a very low-lying $^3\Pi_u$ $(\cdots 2\sigma_g^1 1\pi_u^3)$ first excited state having a calculated term energy (T_e) ranging from 50 to 800 cm^{-1}.[9–12] There are also four singlet states resulting from these same orbital occupancies along with the $(\cdots 1\pi_u^4)$ occupancy predicted to lie within 1.5 eV of the ground state, as with Si_2. On the other hand, relativistic effects are expected to be more important in Ge_2 than Si_2, and Ge_2 is better described in Hund's case (c), where Ω is a good quantum number but Λ and Σ are not.[13,14] Thus the spin–orbit components of the $^3\Pi_u$ state are better described as 0_u^-, 0_u^+, 1_u, and 2_u states (2_u being the lowest-lying), and the $^3\Sigma_g^-$ state is split into the $X0_g^+$ and 1_g states. The energy splitting between the various Ω components of Ge_2 should be substantially larger than in Si_2, for which the splitting between the $^3\Pi_0$ and $^3\Pi_2$ states ($2A$) is 145 cm^{-1},[2,3] and the splitting between the $X0_g^+$ and 1_g components of the $^3\Sigma_g^-$ state (2λ) is 2.6 cm^{-1}.[15]

Prior to the photodetachment studies in our laboratory, the only definitive spectroscopic results on Ge_2 were obtained in a matrix absorption study by Weltner and co-workers.[3] They observed the $^3\Pi_u[1_u(v'=0,1,2,3)] \leftarrow {}^3\Sigma_g^-(X0_g^+)$ transition, finding a term energy of 694 cm^{-1} (711 cm^{-1} between ground vibrational levels of the two states) and a 308 cm^{-1} vibrational frequency for the 1_u component of the $^3\Pi_u$ excited state. This electronic transition is indicated by the solid arrow in Fig. 1. A vibrational frequency assigned to the $^3\Sigma_g^-$ $(X0_g^+)$ state in a matrix was observed in Raman/fluorescence studies.[16] To our knowledge, no spectroscopic information on the low-lying singlet states has until now been obtained. No experimental or *ab initio* results are presently available for Ge_2^-, but if it is electronically similar to Si_2^-, it should have two close-lying $^2\Pi_u(\cdots 2\sigma_g^2 1\pi_u^3)$ and $^2\Sigma_g^+(\cdots 2\sigma_g^1 1\pi_u^4)$ states. For Si_2^-, the $^2\Sigma_g^+$ state was the ground state, and the $^2\Pi_u$ state was approximately 250 ± 80 cm^{-1} higher in energy.[2]

Given the large number of electronic states involved in this study, it is useful to review the selection rules applicable to photodetachment experiments, since these differ markedly from optical spectroscopy. All of the low-lying triplet and singlet valence states of Ge_2 can be generated by removing an electron from a valence orbital of one of the anion states; these one-electron photodetachment transitions are indicated by the arrows in Fig. 1. All of these transitions are allowed in the photoelectron spectrum of Ge_2^-. However, two-electron

[a]Current address: Department of Chemistry, University of California, Los Angeles, CA 90024.
[b]NSERC Postdoctoral Fellow.
[c]Camille and Henry Dreyfus, Teacher–Scholar.

 0021-9606/95/102(18)/6982/8/$6.00

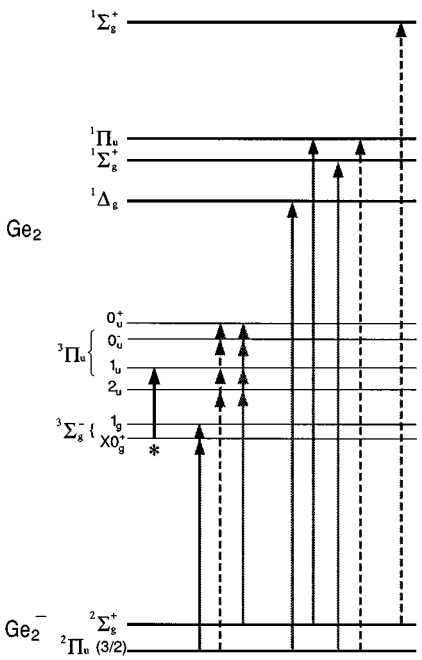

FIG. 1. One-electron photodetachment transitions between the two Ge_2^- and six Ge_2 electronic states discussed in the text. *S*-wave transitions are indicated by solid lines, and *p* wave by dashed lines. The leftmost transition indicated by (*) is that observed by Weltner (Ref. 3) in matrix absorption studies.

transitions, such as the transition from the $^2\Sigma_g^+(\sigma_g^1\pi_u^4)$ anion state to either component of the $^3\Sigma_g^-(\sigma_g^2\pi_u^2)$ neutral are generally too weak to be observed.

The selection rules in ZEKE spectroscopy are more restrictive due to the Wigner threshold law.[17] Near the detachment threshold, the photodetachment cross section goes as

$$\sigma \propto \sigma_0 (E_{h\nu} - E_{\text{threshold}})^{l+1/2}, \tag{1}$$

where $(E_{h\nu}-E_{\text{threshold}})$ and l are the kinetic energy and angular momentum of the ejected electron, respectively. From Eq. (1), it can be seen that the cross section rises sharply above threshold *only* for $l=0$, or *s*-wave electrons. As ZEKE spectroscopy relies on detecting electrons near a detachment threshold, it is sensitive only to *s*-wave transitions. Given the symmetry of the orbitals in a homonuclear diatomic, one can show that only transitions involving the detachment from π_u or σ_u orbitals yield *s*-wave photoelectrons.[18] On the other hand, photodetachment from π_g or σ_g orbitals result in *p*-wave ($l=1$) photoelectrons near threshold. In Fig. 1, those $l>0$ transitions that cannot be observed using ZEKE are indicated as dotted lines. While at times inconvenient, the ZEKE selection rules effectively reveal the orbital from which an electron is ejected in a particular transition, which greatly facilitates spectral assignment.

From the Ge_2^- PES and ZEKE spectra presented here, the splittings (or term energies) between the Ω components are resolved for both the $^3\Sigma_g^-$ and $^3\Pi_u$ states, and the term energies for the $^1\Delta_g$, $(1)^1\Sigma_g^+$ and $^1\Pi_u$ states are extracted. Vibrational frequencies for all of these states are determined from the ZEKE spectrum. The relative energies and vibrational frequencies of the $^2\Pi_u$ (3/2) and the $^2\Sigma_g^+$ anion states are also determined.

II. EXPERIMENT

The apparatus used to obtain the ZEKE spectrum of Ge_2^- has been described in detail elsewhere,[6,19] but the basic operation is as follows. A beam of cold germanium clusters is generated in a molecular beam source similar to that developed by Smalley.[20] The surface of a rotating and translating germanium rod is ablated using 6 mJ/pulse of the second harmonic output of a Nd:YAG laser operated at a 20 Hz repetition rate. The resulting plasma is then entrained in a pulse of 90% Ne/10% He carrier gas from a piezoelectric valve,[21] typically with a backing pressure of 60 to 70 psi. In order to generate sufficient quantities of Ge_2^-, the source was run under conditions that generally produce vibrationally hot ions (e.g., lower beam pulse duration, earlier rod ablation relative to carrier gas entrainment), which results in a mass distribution skewed to lighter masses. The negatively charged species in the subsequent expansion that pass through a 2 mm skimmer are collinearly accelerated to 1 keV, and mass selected using time of flight.[22]

The mass-separated anions then enter a detector region where they are selectively photodetached using an excimer-pumped tunable dye laser. As the dye laser is scanned through the detachment continuum of the ion of interest, only those photoelectrons ejected with nearly zero kinetic energy (ZEKE's) in the frame of the molecular beam are collected as a function of detachment energy. The resulting spectrum is therefore peaked at the thresholds of transitions from anion to neutral levels. This selective detection of threshold electrons, based on techniques developed by Müller-Dethlefs *et al.*[23] for the photoionization of neutrals, yields an energy resolution of 3 cm^{-1}.

The electron signal for the ZEKE spectrum of Ge_2^- was signal averaged for 1500 shots/point, and normalized to the ion current and detachment laser power. The dyes used were Rhodamine 610, Rhodamine 590, Coumarin 540A, Coumarin 503, Coumarin 480, and Coumarin 450.

III. RESULTS

The previously reported photoelectron spectra of Ge_2^- obtained at 2.98 eV photon energy (416 nm) are shown in Fig. 2.[8] The energy resolution is about 10 meV (80 cm^{-1}). Data were taken at polarization angles $\theta=90°$ and $\theta=90°$, where θ is the angle between the electric field polarization vector of the photodetachment laser and the direction in which electrons are detected. The Ge_2^- ZEKE spectrum (solid line) is superimposed onto the $\theta=90°$ PES. The photoelectron spectra are plotted in terms of electron binding energy (in cm^{-1}) to facilitate comparison to the ZEKE spectra.

The photoelectron and ZEKE spectra consist of two distinct bands. Based on Fig. 1 and our previous analysis of Si_2^-,[2] the band at lower binding energy is assigned to transitions to the lowest-lying triplet states of the neutral, and the band at higher binding energy to transitions to the higher-

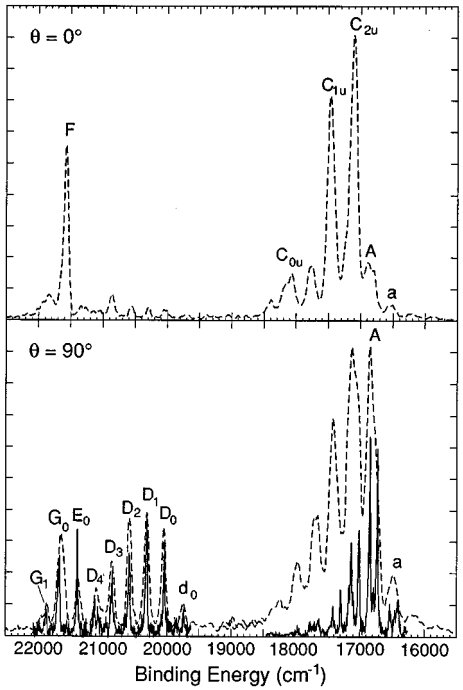

FIG. 2. Photoelectron spectra of Ge_2^- obtained using a 2.98 eV photon energy at two different laser polarizations (dotted lines) and the ZEKE spectrum of Ge_2^- (solid line).

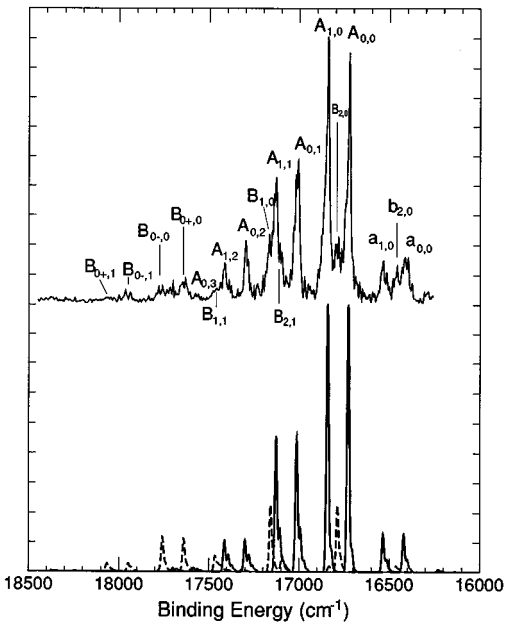

FIG. 3. Top: Triplet band of ZEKE spectrum of Ge_2^-. Bottom: Simulations of the two electronic transitions responsible for structure. Solid line indicates the $^3\Sigma_g^+$ $(1_g, 0_g^+) \leftarrow {}^2\Pi_u$ (3/2) transitions, dashed line indicates the $^3\Pi_u$ $(0_u^\pm, 1_u, 2_u) \leftarrow {}^2\Sigma_g^-$ transitions.

lying singlet neutral states. Within each band, the relative intensities of the peaks in the photoelectron spectra show a strong dependence on θ. For instance, peaks C_{2u}, C_{1u}, and F are particularly intense in the $\theta=0°$ spectrum. Since photoelectrons ejected from different orbitals will generally have different angular distributions,[24] this type of intensity dependence is a signature of multiple anion→neutral electronic transitions contributing to both the triplet and singlet bands. This is entirely consistent with the qualitative energy level pattern in Fig. 1.

Compared to the photoelectron spectra, the peaks in the ZEKE spectrum are considerably narrower, and there is clearly more structure in the triplet band where several peaks in the photoelectron spectrum appear as doublets in the ZEKE spectrum. The peak positions and intensities of the ZEKE spectrum agree considerably better with the PES at $\theta=90°$ than at $\theta=0°$. The upper, solid trace in Fig. 3 shows the triplet band of the ZEKE spectrum on an expanded scale. The peak labeling convention is based on the assignments that will be discussed in detail later. Briefly, different letters correspond to different electronic bands, and where there are two subscripts, the first denotes the value of Ω of the neutral state, and the second is the vibrational quanta in the neutral state (in the singlet band, only the neutral vibrational quanta is denoted in the peak label subscripts). The triplet band is dominated by a progression of doublets labeled $A_{0,v}$ and $A_{1,v}$ $(v=0,1,2,3)$ which have an average splitting of 114 ± 5 cm^{-1}. The centers of the doublets are spaced by 286 ± 5 cm^{-1}; this is presumably a vibrational progression. The peaks in the lower-intensity doublet $a_{0,0}$ and $a_{1,0}$ are found 309 ± 5 cm^{-1} to lower photon energy of peaks $A_{0,0}$ and $A_{1,0}$, respectively. The peak spacing in this doublet is the same as in the $A_{0,v}$ and $A_{1,v}$ progression, so this appears to be a hot band transition from vibrationally excited Ge_2^-.

In addition to these features, there are lower intensity peaks spaced irregularly among the 286 cm^{-1} progression. The most distinct of these is $B_{2,0}$ found 58 ± 7 cm^{-1} to higher photon energy of $A_{0,0}$. Peak $b_{2,0}$ also appears to be a hot band located 326 ± 10 cm^{-1} to lower photon energy of peak $B_{2,0}$. There are also shoulders on both sides of peak $A_{1,1}$ found 308 ± 10 and 374 ± 10 cm^{-1} ($B_{2,1}$ and $B_{1,0}$, respectively) to higher photon energy of peak $B_{2,0}$. Peaks $B_{0^-,0}$ and $B_{0^+,0}$, while appearing to be a part of the $A_{0,v}$ and $A_{1,v}$ progression, are actually spaced by 340 ± 10 cm^{-1} rather than 286 cm^{-1} from peaks $A_{0,2}$ and $A_{1,2}$ (peak $A_{0,3}$, found 80 cm^{-1} to lower photon energy of peak $B_{0^+,0}$, is the next member of the $A_{0,v}$ progression). Peak positions and relative energies are summarized in Table I. The peak positions generally have an uncertainty of ±5 cm^{-1}, and so the relative energies are good to ±7 cm^{-1}.

The ZEKE spectrum of the singlet band of Ge_2^- is shown on an expanded scale as the solid trace in Fig. 4. There appear to be three electronic transitions contributing to the structure in this region. The lowest energy transition consists of a progression labeled D_v $(v=0, ..., 4)$. This progression is long enough to extract an anharmonicity; we find $\omega_e=276\pm3$ cm^{-1} and $\omega_e x_e=1.2\pm0.6$ cm^{-1}. The origin, D_0, is found 3314 cm^{-1} above peak $A_{0,0}$ in the singlet band. Peak d_0 appears to be a hot band, and is found 307 ± 7 cm^{-1} to lower photon energy of D_0. E_0 indicates the origin of a second electronic transition found 4664 cm^{-1} to higher photon energy of peak $A_{0,0}$. Peak G_0, is spaced approximately 280 cm^{-1} to higher photon energy of peak E_0, which could reasonably be a vibrational spacing. However, peak E_2, which is found 607 ± 7 cm^{-1} from E_0, is much less intense

TABLE I. Peak positions, relative energies, and assignments in both the PES and ZEKE spectra. The asterisk (*) indicates that the peak was observed only in the PES. In the case where peaks are observed in both spectra, the detachment energy obtained from the ZEKE spectrum is used. It should be noted that 2_u, 1_u, 0_u^+, and 0_u^- refer to the Ω components of the $^3\Pi_u$ neutral state, and 0_g^+ and 1_g are the components of the $^3\Sigma_g^-$ neutral state.

Peak	Binding energy (cm^{-1})	Relative energy (cm^{-1})	Assignment neutral$+e-(eKE\approx 0)\leftarrow$anion
$a_{0,0}$	16 409	−318	$0_a^+(v'=0)\leftarrow{}^2\Pi_{u.3/2}(v''=1)$
$b_{2,0}$	16 451	−268	$2_u(v'=0)\leftarrow{}^2\Sigma_g^+(v''=1)$
$a_{1,0}$	16 534	−193	$1_a(v'=0)\leftarrow{}^2\Pi_{u.3/2}(v''=1)$
$A_{0,0}$	16 727	0	$0_g^+(v'=0)\leftarrow{}^2\Pi_{u.3/2}(v''=0)$
$B_{2,0}$	16 785	58	$2_u(v'=0)\leftarrow{}^2\Sigma_g^+(v''=0)$
$A_{1,0}$	16 840	113	$1_g(v'=0)\leftarrow{}^2\Pi_{u.32}(v''=0)$
$*C_{2u}$		~280	$2_u(v'=0)\leftarrow{}^2\Pi_{u.3/2}(v''=0)$
$A_{0,1}$	17 009	282	$0_g^+(v'=1)\leftarrow{}^2\Pi_{u.3/2}(v''=0)$
$B_{2,1}$	17 103	376	$2_u(v'=1)\leftarrow{}^2\Sigma_g^+(v''=0)$
$A_{1,1}$	17 129	402	$1_g(v'=1)\leftarrow{}^2\Pi_{u.3/2}(v''=0)$
$B_{1,0}$	17 159	432	$1_u(v'=0)\leftarrow{}^2\Sigma_g^+(v''=0)$
$A_{0,2}$	17 300	573	$0_g^+(v'=1)\leftarrow{}^2\Pi_{u.3/2}(v''=0)$
$*C_{1u}$		~670	$1_u(v'=0)\leftarrow{}^2\Pi_{u.3/2}(v''=0)$
$A_{1,2}$	17 417	690	$1_g(v'=2)\leftarrow{}^2\Pi_{u.3/2}(v''=0)$
$B_{1,1}$	17 467	740	$1_u\ (v'=1)\leftarrow{}^2\Sigma_g^+(v''=0)$
$A_{0,3}$	17 580	853	$0_g^+(v'=3)\leftarrow{}^2\Pi_{u.3/2}(v''=0)$
$B_{0+,0}$	17 641	914	$0_u^+(v'=0)\leftarrow{}^2\Sigma_g^+(v''=0)$
$B_{0-,0}$	17 753	1026	$0_u^-(v'=0)\leftarrow{}^2\Sigma_g^+(v''=0)$
$*C_{0u}$		~1200	$0_u^\pm(v'=0)\leftarrow{}^2\Pi_{u.3/2}(v''=0)$
$B_{0+,1}$	17 966	1239	$0_u^+(v'=1)\leftarrow{}^2\Sigma_g^+(v''=0)$
$B_{0-,1}$	18 067	1340	$0_u^-(v'=1)\leftarrow{}^2\Sigma_g^+(v''=0)$
d_0	19 734	3007	$^1\Delta_g\ (v'=0)\leftarrow{}^2\Pi_{u.3/2}(v''=1)$
D_0	20 040	3313	$^1\Delta_g\ (v'=0)\leftarrow{}^2\Pi_{u.3/2}(v''=0)$
D_1	20 312	3585	$^1\Delta_g\ (v'=0)\leftarrow{}^2\Pi_{u.3/2}(v''=0)$
D_2	20 586	3859	$^1\Delta_g\ (v'=2)\leftarrow{}^2\Pi_{u.3/2}(v''=0)$
D_3	20 846	4119	$^1\Delta_g\ (v'=3)\leftarrow{}^2\Pi_{u.3/2}(v''=0)$
e_0	21 062	4335	$^1\Pi_u\ (v'=0)\leftarrow{}^2\Sigma_g^+(v''=1)$
D_4	21 119	4392	$^1\Delta_g\ (v'=4)\leftarrow{}^2\Pi_{u.3/2}(v''=0)$
E_0	21 390	4664	$^1\Pi_u(v'=0)\leftarrow{}^2\Sigma_g^+(v''=0)$
g_1	21 552	4825	$(1)^1\Sigma_g^+(v'=1)\leftarrow{}^2\Pi_{u.3/2}(v''=1)$
$*F$		~4940	$^1\Pi_u(v'=0)\leftarrow{}^2\Pi_{u.3/2}(v''=0)$
G_0	21 668/21 690	4941/4963	$(1)^1\Sigma_g^+(v'=0)\leftarrow{}^2\Pi_{u.3/2}\ (v''=0)$; $^1\Pi_u(v'=1)\leftarrow{}^2\Sigma_g^+(v''=0)$
g_2	21 784	5057	$(1)^1\Sigma_g^+(v'=2)\leftarrow{}^2\Pi_{u.3/2}(v''=1)$
G_1	21 872	5145	$(1)^1\Sigma_g^+(v'=1)\leftarrow{}^2\Pi_{u.3/2}(v''=0)$
E_2	21 997	5271	$^1\Pi_u\ (v'=2)\leftarrow{}^2\Sigma_g^+(v''=0)$

than would be expected if E_0, G_0 and E_2 formed a progression. On the other hand, peak G_0 is broad, and it is more likely that two transitions are contributing to G_0: the 1–0 (i.e., $v'=1\leftarrow v''=0$) member of the E_0 progression, and the origin of another electronic band for which G_1 is the 1–0 transition. This gives a vibrational frequency of 303 ± 5 cm^{-1} for the neutral state corresponding to the peaks E_j, and 204 ± 7 cm^{-1} for the state corresponding to peaks G_j. Peak e_0, another hot band, lies 329 ± 7 cm^{-1} from E_0. Peaks g_1 and g_2 are spaced approximately 100 cm^{-1} to lower photon energy of G_0 and G_1, respectively. As the anion frequencies so far have been either approximately 309 or 326 cm^{-1}, peaks g_1 and g_2 are spaced appropriately to be the 1–1 and 2–1 sequence and hot band transitions, respectively, between an anion state and the neutral state responsible for G_0. Again, Table I summarizes peak positions and relative energies.

Several of the most intense peaks in the PES at $\theta=0°$ that are missing in the $\theta=90°$ spectrum are also absent in the ZEKE spectrum. Specifically, the three peaks C_Ω do not appear in the triplet band. Based on the discussion in Sec. I, we expect that these are p-wave transitions that will not contribute to the ZEKE spectrum. Peak F in the singlet band of the PES has the same intensity dependence as the C_Ω peaks and should therefore also involve p-wave detachment. There is, however, a feature in the ZEKE spectrum, G_0, that lies close to the energy of peak F. Upon close inspection of peak of the lower panel of Fig. 2, peak G_0 does appear to lie to somewhat higher energy than peak F. It therefore seems likely that peak F in the photoelectron spectrum is composed of two transitions, one of which proceeds via s-wave photodetachment, yielding peak G_0 in the ZEKE spectrum, and the other via p-wave detachment, which does not appear in the ZEKE spectrum.

IV. ANALYSIS AND DISCUSSION

The assignment and subsequent analysis of the spectra requires consideration of both the ZEKE spectra and the

PES. The approach taken below is to first analyze the triplet band of the PES and ZEKE spectrum considering also the spectroscopic information from Weltner's matrix studies on Ge_2. From this, spectroscopic constants of the anion states will be extracted. With more information about the anion states, the analysis of the singlet band then proceeds in a straightforward manner.

A. Triplet band

Figure 1 illustrates the three one-electron transitions between the doublet anion states and triplet neutral states, two of which should be observed in the ZEKE spectrum (Fig. 3): the $^3\Sigma_g^-\ (1_g, X0_g^+) \leftarrow {}^2\Pi_u(3/2)$ transition and the $^3\Pi_u\ (0^+, 0^-, 1_u, 2_u) \leftarrow {}^2\Sigma_g^+$ transitions. We can immediately assign peaks $A_{\Omega,v}$ to the former. As pointed out by Weltner,[3] the zero field splitting (ZFS) between the $X0_g^+$ and 1_g components of the neutral $^3\Sigma_g^-$ state of Ge_2 is expected to be approximately 100 cm^{-1} based on the square of the spin–orbit splittings in the Ge and Si atoms ($SO_{Ge}/SO_{Si}=6.3$) and the ZFS in Si_2 (2.6 cm^{-1}).[15] It is therefore reasonable to associate the $A_{0,v}-A_{1,v}$ doublet structure, for which the average spacing is 117 cm^{-1}, with the ZFS between the $X0_g^+$ and 1_g components of the neutral $^3\Sigma_g^-$ state. This splitting has contributions from both the first order spin–spin interaction and the second order spin–orbit interaction (with the low-lying $^1\Sigma_g^+$ state),[14] but as the former is generally on the order of less than 1 cm^{-1},[25] 117 cm^{-1} can be taken as the second-order spin–orbit constant (conventionally, $2\lambda^{SO}$). The 286 cm^{-1} vibrational frequency characteristic of the $A_{\Omega,v}$ progression is slightly higher than the 277 ($\pm\sim10$; error bars were not included in the spectral analysis) cm^{-1} ground state frequency determined from Raman matrix studies.[16] From the position of the hot bands (peaks $a_{0,0}$ and $a_{1,0}$) we determine that the frequency of the $^2\Pi_u$ anion is 309 cm^{-1}.

From the Si_2-ZEKE spectrum,[2] we were also able to determine the 122 cm^{-1} spin–orbit splitting in the $^2\Pi_u$ anion, because the population of the $\Omega=1/2$ level in the ion beam was sufficient for us to observe the $^3\Sigma_g^- \leftarrow {}^2\Pi_u\ (1/2)$ transition in addition to the $^3\Sigma_g^- \leftarrow {}^2\Pi_u\ (3/2)$ transition. However, since the Ge_2^- spin–orbit splitting is expected to be roughly 700 to 800 cm^{-1}, the population of spin–orbit excited anions in the beam is likely to be very small, and we only observe transitions from the $\Omega=3/2$ component.

We can simulate the vibrational structure in the $^3\Sigma_g^-\ (0_g^+, 1_g) \leftarrow {}^2\Pi_u\ (3/2)$ transitions within the Franck–Condon approximation. In the simulation, we assume that the intensity of individual vibronic transitions within an electronic band are proportional to their Franck–Condon factors (FCF's),

$$\text{Intensity} \propto |\langle v' | v'' \rangle|^2. \tag{2}$$

The vibrational wave functions of the neutral and anion, $|v'\rangle$ and $|v''\rangle$, respectively, are taken to be harmonic (or Morse) oscillators with the frequencies determined from the spectra. The relative bond distances of the anion and neutral are then varied until the extension of the simulated progression matches the observed progression.

The simulation of the $^3\Sigma_g^-\ (0_g^+, 1_g) \leftarrow {}^2\Pi_u\ (3/2)$ transitions is shown as the lighter dashed trace on the lower part of Fig. 3. Harmonic oscillator wave functions with 309 and 286 cm^{-1} frequencies were used for the anion and neutral, respectively. A bond distance difference of 0.059 ± 0.003 Å was required to reproduce the extension of the progression, and while the direction of the bond length change cannot be determined from the simulation (using harmonic oscillators) the anion bond length should be shorter than the neutral, as the transition involves removing a bonding electron. An anion vibrational temperature of 350 K was required to match the hot band intensity; this temperature is fairly typical for our cluster source given this vibrational frequency.

Given the $^3\Sigma_g^+\ (0_g^+, 1_g) \leftarrow {}^2\Pi_u\ (3/2)$ assignment and the term energy of the $^3\Pi_u\ (1_u)$ state from Weltner's matrix studies, we would expect the $^3\Pi_u(1_u) \leftarrow {}^2\Pi_u\ (3/2)$ transition to lie approximately 700 cm^{-1} above the $^3\Sigma_g^+\ (X0_g^+) \leftarrow {}^2\Pi_u\ (3/2)$ transition. This will be observed only in the PES as it involves the removal of a σ_g electron and should proceed by p-wave detachment near threshold. In the upper panel of Fig. 2, peak C_{1u} lies 670 ± 50 cm^{-1} to higher energy than peak A. We therefore assign peak C_{1u} in the PES to the $^3\Pi_u\ (1_u) \leftarrow {}^2\Pi_u\ (3/2)$ transition. It then follows that peak C_{2u}, found 360 cm^{-1} to lower energy, is the $^3\Pi_u\ (2_u) \leftarrow {}^2\Pi_u\ (3/2)$ transition. We tentatively assign peak C_{0u}, 890 cm^{-1} to higher energy C_{2u}, to the $^3\Pi_u\ (0_u^-) \leftarrow {}^2\Pi_u\ (3/2)$ and $^3\Pi_u\ (0_u^+) \leftarrow {}^2\Pi_u\ (3/2)$ transitions; this is discussed further below. The peak between C_{1u} and C_{0u} in the $\theta=\theta^\circ$ spectrum may be the $^3\Pi_u\ (1_u)(v'=1) \leftarrow {}^2\Pi_u\ (3/2)$ transition.

We next consider the remaining structure in the triplet region of the ZEKE spectrum that has not been accounted for by the $^3\Sigma_g^-\ (X0_g^+, 1_g) \leftarrow {}^2\Pi_u\ (3/2)$ transition. Peaks $B_{\Omega,v}$ must result from the $^3\Pi_u\ (0_u^-, 0_u^+, 1_u, 2_u) \leftarrow {}^2\Sigma_g^+$ transitions, the only others that can proceed via s-wave detachment in this energy region. By comparing the dotted trace of the simulation with the ZEKE spectrum, the lower-intensity peaks and shoulders labeled $B_{\Omega,v}$ stand out more clearly as a second set of electronic transitions. The most distinct of these peaks is $B_{2,0}$. The shoulder $B_{1,0}$ is found 374 cm^{-1} to higher photon energy, which is close to the $^3\Pi_u\ (2_u-1_u)$ splitting observed in the PES (i.e., the spacing between peaks C_{2u} and C_{1u}). Moreover, $B_{2,1}$ and $B_{1,1}$ are found approximately 308 cm^{-1} to higher photon energy of $B_{2,0}$ and $B_{1,0}$, respectively, which is the vibrational frequency of the $^3\Pi_u\ (1_u)$ state determined by Weltner. We therefore assign peak $B_{2,0}$ to the $^3\Pi_u\ (2_u) \leftarrow {}^2\Sigma_g^+$ transition, and $B_{1,0}$ to the $^3\Pi_u\ (1_u) \leftarrow {}^2\Sigma_g^+$ transition. Peaks $B_{2,1}$ and $B_{1,1}$ are transitions to the $v'=1$ levels of the $^3\Pi_u\ (2_u)$ and $^3\Pi_u\ (1_u)$ states, respectively.

The relative energies of the $^2\Sigma_g^+$ and $^2\Pi_u\ (3/2)$ anion states can now be determined. The $^3\Pi_u\ (1_u) \leftarrow {}^2\Sigma_g^+$ transition (peak $B_{1,0}$) is 432 ± 10 cm^{-1} higher in energy than the $^3\Sigma_g^-(X0_g^+) \leftarrow {}^2\Pi_u\ (3/2)$ transition (peak $A_{0,0}$). From Weltner's work, the $^3\Pi_u\ (1_u)\ v=0$ level is known to lie 711 ± 3 cm^{-1} above the $^3\Sigma_g^-\ (X0_g^+)\ v=0$ level.[3] This means that for the anion, the $^2\Pi_u\ (3/2)$ level is 279 ± 11 cm^{-1} *below* the $^2\Sigma_g^+$ level. (By using Weltner's value, the energy splitting we determine for the anion states is more accurate than what we would have determined from comparing the position of peak C_{2u} in the PES and peak $B_{2,0}$ in the ZEKE spectrum, which would have yielded 240 ± 80 cm^{-1}.) The relative weakness of

the B transitions likely results from their originating from an excited anion level. Given the expected spin–orbit splitting in the $^2\Pi$ state of Ge_2^-, the $^2\Pi_u$ (1/2) excited level may be roughly 400 to 500 cm^{-1} *above* the $^2\Sigma_g^+$ state. The vibrational frequency of the $^2\Sigma_g^+$ state is given from the position of the $b_{2,0}$ hot band, which is found 326 cm^{-1} to lower photon energy of peak $B_{2,0}$. This is slightly higher than 309 cm^{-1} frequency determined for the $^2\Pi_u$ (3/2) state.

So far, the peaks labeled $B_{0+,0}$ and $B_{0-,0}$ have not been addressed. These are approximately half the intensity of peak $B_{2,0}$, and they are spaced 856 and 968 cm^{-1}, respectively, to higher photon energy, although the location of peak $B_{0-,0}$ is difficult to determine accurately. As there are no other electronic transitions that should be observed in this region of the ZEKE spectrum, we tentatively assign them to the $^3\Pi_{0u}(0_u^+)\leftarrow{}^3\Sigma_g^+$ and $^3\Pi_0(0_u^-)\leftarrow{}^2\Sigma_g^+$ transitions, respectively. This assignment is consistent with the observation that the average spacing of these two peaks from peak $B_{2,0}$, 912 cm^{-1}, is very close to the 890 cm^{-1} spacing between peaks C_{2u} and peaks C_{0u} in the PES. The major cause of the splitting of the $^3\Pi_{0u}$ level is from second-order spin–orbit coupling of either the + or − parity component to a nearby Σ_u state.[26] The electronic spectroscopy of Si_2 reveals a relatively low-lying (~3 eV) $^3\Sigma_u^-$ state,[27] and if an analogous state is responsible for the perturbation in Ge_2, it will repel the 0_u^+ level which will then lie slightly below the 0_u^- level.

Assuming these peaks do represent the $^3\Pi_u(0_u^\pm)\leftarrow{}^2\Sigma_g^+$ transitions, the spin–orbit coupling constant, Am for the $^3\Pi_u$ state is 484 cm^{-1} (i.e., one-half the $2_u-0_u^-$ splitting) which is considerably higher than the 2_u-1_u splitting, 374 cm^{-1}. The asymmetric arrangement of the $^3\Pi_u$ $(0_u^\pm)$ and $^3\Pi_u$ (2_u) states about the $^3\Pi_u$ (1_u) state was also observed to a lesser extent for the Si_2 $^3\Pi_u$ state in Weltner's studies, and is due to the mixing of the $\Omega=1$ level with the higher-lying $^1\Pi_u$ state. This mixing will be further addressed in the next section where the term energy of the $^1\Pi_u$ state is discussed.

Simulations of the $^3\Pi_u$ $(0_u^-,0_u^+,1_u,2_u)\leftarrow{}^2\Sigma_g^+$ transitions are shown in the lower half of Fig. 3 (heavier dashed line). The neutral frequency assumed for all four components was 308 cm^{-1}, and the anion frequency was assumed to be 326 cm^{-1}. The transitions to the $^3\Pi_u$ $(0_u^\pm)$ states were assumed to be half the intensity of the transitions to the $^3\Pi_u$ (1_u) and $^3\Pi_u$ (2_u) states, which were in turn scaled to have 0.25 the intensity of the $^3\Sigma_g^-$ $(X0_g^+)\leftarrow{}^2\Pi_u$ (3/2) transition in order to best match the spectrum. A bond length difference of 0.04 Å between the anion and neutral was assumed to match the extent of the vibrational progression, and again, the anion should have the shorter bond distance. This bond length changes should be regarded as quite approximate given the most of these transitions are only partially resolved.

Geometry calculations on the lowest-lying neutral states predict the bond length of the $^3\Pi_u$ excited state to be 0.1 Å *shorter* than the $^3\Sigma_g^-$ state; calculations yield values from 2.42 to 2.46 Å for the $^3\Sigma_g^-$ state and 2.33 to 2.39 Å for the $^3\Pi_u$ state.[9–12] Taking into account the bond length differences determined from the spectra, this suggests that the anion $^2\Pi_u$ state is approximately 0.8 Å *longer* than the $^2\Sigma_g^+$ state. Thus, shifting an electron from the σ_g to the π_u orbital results in shortening the bond by nearly 0.1 Å in both the anion and neutral. The relative bond distances between the anion and neutral states are startlingly similar to those found for Si_2 and Si_2^-. The anion states were found to be different by 0.09 Å with the $^2\Pi_u$ state being longer, and the neutral states were known to be different by 0.09 Å with the $^3\Sigma_g^-$ state being longer. Moreover, spectral simulations of the ZEKE spectrum of Si_2^- gave bond length differences on the order of 0.04 Å in both ZEKE transitions. This interesting similarity between the response of the bond lengths of Ge_2 and Si_2 to the shifting of valence electrons within the triplet manifold further reflects the electronic similarity between these two species.

Table I summarizes the peak assignments discussed in this section, and Table II summarizes the spectroscopic constants extracted from the spectrum and used in the spectral simulations, including the term energies of the $^3\Pi_u$ $(0_u^-,0_u^+,1_u,2_u)$ states used in the spectral simulation.

B. Singlet band

Electronic structure calculations[9] predict that the $^1\Delta_g$, $(1)^1\Sigma_g^+$ and $^1\Pi_u$ neutral states lie roughly 0.5–0.7 eV above the ground state, and transitions to these states should result in the structure observed to higher energy in both the PES and ZEKE spectrum. In Table II, the *ab initio* term energies of these three states are listed. Figure 1 shows the four one-electron transitions between the two anion states and these three neutral states. An additional $(2)^1\Sigma_g^+$ state is predicted to lie approximately 1.3 eV above the ground state; the (2) $^1\Sigma_g^+\leftarrow{}^2\Sigma_g^+$ (p wave) transition is not observed in the PES obtained using 2.98 eV photon energy, but in the PES obtained using 4.66 eV photon energy, it was found to lie (with lower accuracy) 9300 ± 100 cm^{-1} (1.15 eV) above the $^3\Sigma_g^-\leftarrow{}^2\Pi_u$ (3/2) transition. Adding the term energy of the $^2\Sigma_g^+$ anion state yields $T_e=9580$ cm^{-1} for the $(2)^1\Sigma_g^+$ state. There are three transitions expected to be observed in the ZEKE spectrum, $^1\Delta_g\leftarrow{}^2\Pi_u$ (3/2), $(1)^1\Sigma_g^+\leftarrow{}^2\Pi_u$ (3/2), and $^1\Pi_u\leftarrow{}^2\Sigma_g^+$.

Since the $^1\Delta_g$ state is predicted to be the lowest-lying of the singlet states, peaks $D_v(v=0,\ldots,4)$ are assigned to the $^1\Delta_g(v'=0,\ldots,4)\leftarrow{}^2\Pi_u$ (3/2) transition. The 276 ± 3 cm^{-1} ($\omega_e\chi_e=1.2\pm0.6$ cm^{-1}) progression is the most extended of all the progressions. This is consistent with calculated geometries, which predict the $^1\Delta_g$ state to have the longest bond distance of all the low-lying states. The position of the hot band, d_0, gives an anion frequency of approximately 308 cm^{-1}, which further supports that this is a transition from the $^2\Pi_u$ (3/2) anion state. The energy spacing between peak D_0 and $A_{0,0}$ directly gives the term energy of the $^1\Delta_g$ state: 3314 ± 7 cm^{-1}.

As with the triplet band, the Franck–Condon simulation gives an approximate bond length difference between the anion and neutral. The total simulation of the singlet band is shown as the dashed line in Fig. 4. In the case of the transition to the $^1\Delta_g$ state, the bond length difference is determined to be 0.095 ± 0.005 Å. This further suggests that the bond distance in the $^1\Delta_g$ state is 0.036 Å longer than that in the $^3\Sigma_g^-$ $(X0_g^+)$ state. This is in qualitative agreement with the difference in the calculated bond distances between these two states, 0.06 Å.[9]

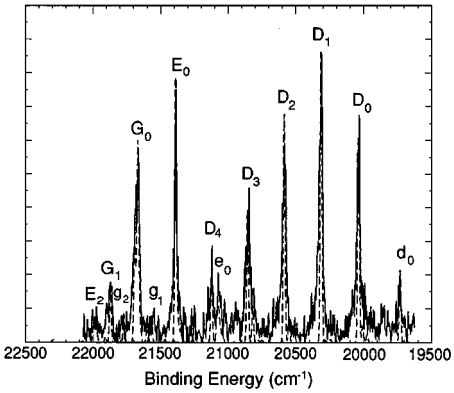

FIG. 4. Singlet band of ZEKE spectrum of Ge_2^- (solid line) and spectral simulations (dotted line, see the text).

Again referring to the calculated frequencies of the singlet states (Table II), the $(1)^1\Sigma_g^+$ state has a substantially lower frequency than the other singlet states. We therefore assign the G_0-G_1 progression to the $(1)^1\Sigma_g^+\leftarrow{}^2\Pi_u$ (3/2) transition, as it exhibits the smallest vibrational spacing, 204 cm^{-1}. From the average spacing of the sequence bands, g_1 and g_2, the anion frequency in this transition is approximately 305 cm^{-1}, which is close to the previously determined $^2\Pi_u$ (3/2) frequency, further supporting the assignment. As above, the term energy of the $(1)^1\Sigma_g^+$ state can be extracted from the energy spacing between peaks G_0 and $A_{0,0}$: 4941 cm^{-1}. For the simulation in Fig. 4, a bond length difference of 0.045 ± 0.005 Å was found to satisfactorily fit the progression. This is only 0.014 Å less than that used in the $^3\Sigma_g^-$ $(X0_g^+)\leftarrow{}^2\Pi_u$ (3/2) fit, suggesting that the bond distances of the ground $^3\Sigma_g^-$ $(X0_g^+)$ and excited $(1)^1\Sigma_g^+$ states have nearly identical bond distances. While this is counterintuitive given the lower frequency in the excited singlet state, geometry calculations do predict these two states to have nearly identical bond lengths, presumably because the $(1)^1\Sigma_g^+$ state is a mixture of both the $1\pi_u^4$ and $2\sigma_g^2 1\pi_u^2$ configurations, and population in the $1\pi_u$ orbital results in a shorter bond distance.[9–12]

The remaining vibrational progression in the ZEKE spectrum, E_v, can be assigned by elimination to the $^1\Pi_u\leftarrow{}^2\Sigma_g^+$ transition. The position of the hot band, e_0, gives an anion frequency of 329 ± 5 cm^{-1}, which is in agreement with the 326 ± 5 cm^{-1} determined for the $^2\Sigma_g^+$ anion state determined from the triplet band. For the simulation in Fig. 4, the neutral frequency was chosen as 304 ± 5 cm^{-1} with a bond length change between the anion and neutral of 0.050 ± 0.005 Å.

In order to determine the term energy of the $^1\Pi_u$ state, we must add the term energy of the $^2\Sigma_g^+$ anion state to the energy separation between peak E_0 and $A_{0,0}$, which gives a value of 4943 cm^{-1}, virtually identical to the term energy of the (1) $^3\Sigma_g^+$ state! Within the error bars of the experiment, we cannot assert which of the $(1)^1\Sigma_g^+$ and $^1\Pi_u$ states is higher lying, and calculations do not give a strong indication; the $(1)^1\Sigma_g^+$ and the $^1\Pi_u$ states are predicted to close lying, with Balasubramanian[9] and Pacchioni[11] predicting the $^1\Pi_u$ state to be higher-lying than the $(1)^1\Sigma_g^+$ state, and Kingcade *et al.*[12] predicting the $^1\Pi_u$ state to be lower. This remarkable near degeneracy of electronic states is further supported by the sole *p*-wave transition observed in the singlet band of the PES (Fig. 2). Peak *F* in the PES, which can only be the $^1\Pi_u\leftarrow{}^2\Pi_u$ (3/2) transition, energetically coincides with peak G_0 in the ZEKE spectrum, which, in addition to irrefutably being an *s*-wave transition, has been definitively assigned to the $(1)^1\Sigma_g^+\leftarrow{}^2\Pi_u$ (3/2) transition. Since the coincident tran-

TABLE II. Spectroscopic constants of the low-lying electronic states of Ge_2 and Ge_2^-.

	State		Orbital occupancy[a]	T_e (cm^{-1})	ω_e (cm^{-1})	r_e (Å)	*ab initio* T_e/ω_e[a]
	$(2)^1\Sigma_g^+$		$1\pi^4$ (51%) $2\sigma_g^2 1\pi_u^2$ (17%) $1\pi_u^2 1\pi_g^2$ (14%)	9578[b]	⋯	⋯	10 840/258
	$^1\Pi_u$		$2\sigma_a 1\pi_u^3$ (80%)	4943	303 ± 5	$y+$ 0.05	5794/269
	$(1)^1\Sigma_g^+$		$2\sigma_g^2 1\pi_u^2$ (63%) $1\pi^4$ (17%)	4941	204 ± 7	$x+$ 0.045	5521/192
	$1\Delta_g$		$2\sigma_g^2 1\pi_u^2$ (83%)	3308	276 ± 3	$x+$ 0.095	3982/255
Ge_2	$^3\Pi_u$	0_u^-	$2\sigma_g 1\pi_u^3$ (80%)	1305	308[3]	y^+	767/251
		0_u^+		1193		0.04	
		1_u		711[3]			
		2_u		337			
	$^3\Sigma_g^-$	1_a	$2\sigma_g^2 1\pi_u^2$ (85%)	114	286 ± 5	$x+$ 0.059	0/259
		0_a					
	$^2\Sigma_g^+$		$2\sigma_g 1\pi_u^4$	279 ± 10	326 ± 10	y	
Ge_2^-							
	$2\Pi_{u.3/2}$		$2\sigma_g^2 1\pi_u^3$	0	309 ± 5	x	

[a]Reference 9.
[b]Value obtained from 4.66 eV PES of Ge_2^- with ±100 cm^{-1} uncertainty.

sitions originate from the same anion state, the neutral states must coincide energetically.

Given the term energies of the $^1\Pi_u$ and $(1)^1\Sigma_g^+$ states, we can calculate the strengths of the various perturbations in the triplet manifold and compare them with experiment. For example, the zero field splitting, $2\lambda_{SO}$, between the $X0_g^+$ and 1_g levels of the $^3\Sigma_g^-$ state is caused primarily by second order spin–orbit coupling between the parent $^3\Sigma_g^-$ and $^1\Sigma_g^+$ states[14]

$$2\lambda^{SO}=\frac{|\langle^3\Sigma_{0g}^-|H_{SO}|^1\Sigma_g^+\rangle|^2}{E(^1\Sigma_g^+)-E(^3\Sigma_g^-)}. \tag{3}$$

The matrix element in the numerator is given by $-2A$, where A is the spin–orbit coupling constant for the $^3\Pi_u$ state. The measured zero field splitting is 117 cm^{-1}, and the energy splitting in the denominator is 4824 cm^{-1}, yielding $A=371$ cm^{-1}. This is lower than, but on the same order of the experimental value of 484 cm^{-1}.

In a similar vein, the extent of the asymmetry between the $^3\Pi_u$ $(2_u,1_u,0_u^+)$ levels is largely due to the repulsion between the $^1\Pi_u$ and $^3\Pi_u$ (1_u) levels through spin–orbit coupling, and can be calculated given the term energy of the $^1\Pi_u$ state. The shift to both states is given by[14] $A^2/2K$, where $2K$ is the deperturbed splitting between the $^3\Pi_u$ (1_u) and $^1\Pi_u$ levels [i.e., the $(^3\Pi_u-^1\Pi_u)$ exchange integral]. In the absence of this spin–orbit effect, the term energy for the $^3\Pi_u$ state would be 821 cm^{-1} (halfway between the 2_u and 0_u^- states) rather than at 711 cm^{-1}, and the $^1\Pi_u$ state would lie accordingly lower in energy, so that the deperturbed exchange $K=4012$ cm^{-1}. Using $A=484$ cm^{-1}, we find $A^2/2K=59$ cm^{-1}. This is in the range of but smaller than the experimental asymmetry, 110 cm^{-1}, suggesting that the 1_u state is interacting with more than one higher-lying electronic state. This is certainly plausible given the electronic complexity of Ge_2; there are likely to be multiple electronic states not too far beyond the energies explored in our experiments.

V. CONCLUSION

The work presented here again shows how the combination of anion PES and ZEKE spectroscopy provides a powerful probe of electronically complicated species. We have determined term energies and vibrational frequencies for the five lowest-lying neutral triplet and singlet states of Ge_2 and for the $^2\Pi_u$ (3/2) and $^2\Sigma_g^+$ states of Ge_2^-. These assignments were facilitated by previous *ab initio* calculations on Ge_2 as well as Weltner's term energy for the $^3\Pi_u$ (1_u) state. A comparison with Si_2 and Si_2^- shows clearly the increasing importance of relativistic effects, namely, stronger spin-orbit interactions, in Ge_2 and Ge_2^-.

From the triplet band of the ZEKE spectrum, the zero field splitting between the $X0_g^+$ and 1_g components of the $^3\Sigma_g^-$ neutral state was determined to be 114 ± 5 cm^{-1}, both components having a 286 ± 5 cm^{-1} vibrational frequency. The term energies of the 2_u, 1_u, 0_u^+, and 0_u^- components of the $^3\Pi_u$ state were found to be 337, 711, 1193, and 1305 ± 14 cm^{-1}, respectively. These energies are taken with respect to the zero-point energies. The vibrational frequency for the 2_u and 1_u components in 308 cm^{-1}, in agreement with Weltner's value for the 1_u component. It was also determined that the $^2\Sigma_g^+$ ($\omega_e=326\pm10$ cm^{-1}) anion state lie 279 ± 10 cm^{-1} above the $^2\Pi_u$ (3/2) ($\omega_e=309\pm5$ cm^{-1}) level.

From the singlet band, term energies for the $^1\Delta_g$, (1) $^1\Sigma_g^+$, and $^1\Pi_u$ states were determined. The $^1\Delta_g$ ($\omega_e=276\pm3$ cm^{-1}), as predicted, was found to be the lowest lying with $T_e=3308\pm7$ cm^{-1}. The $(1)^1\Sigma_g^+$ ($\omega_e=204\pm7$ cm^{-1}) and $^1\Pi_u$ ($\omega_e=304\pm10$ cm^{-1}) states are nearly degenerate, with T_e's around 4942 ± 7 cm^{-1}.

ACKNOWLEDGMENT

This work has been supported under NSF Grant No. DMR-9201159.

[1] P. J. Bruna, S. D. Peyerimhoff, and R. J. Buenker, J. Chem. Phys. **72**, 5437 (1980); A. D. McLean, B. Liu, and G. S. Chandler, *ibid.* **80**, 5130 (1984); K. Raghavachari, *ibid.* **84**, 5672 (1986); C. W. Bauschlicher, Jr. and S. R. Langhoff, *ibid.* **87**, 2919 (1987); H. P. Lüthi and A. D. McLean, Chem. Phys. Lett. **135**, 352 (1987); F. Müller-Plathe and L. Laaksonen, *ibid.* **160**, 175 (1989); K. Raghavachari and C. M. Rohlfing, J. Chem. Phys. **94**, 3670 (1991).
[2] T. N. Kitsopoulos, C. J. Chick, Y. Zhao, and D. M. Neumark, J. Chem. Phys. **95**, 1441 (1991); C. C. Arnold, T. N. Kitsopoulos, and D. M. Neumark, *ibid.* **99**, 766 (1993).
[3] S. Li, R. J. Van Zee and W. Weltner, Jr., J. Chem. Phys. **100**, 7079 (1994).
[4] S. Li, R. J. Van Zee, and W. Weltner, Jr., J. Phys. Chem. **97**, 11393 (1993); **98**, 2275 (1994).
[5] C. Xu, E. de Beer, D. W. Arnold, C. C. Arnold, and D. M. Neumark, J. Chem. Phys. **101**, 5406 (1994); C. C. Arnold and D. M. Neumark, Can. J. Phys. **72**, 1322 (1994).
[6] T. N. Kitsopoulos, C. J. Chick, A. Weaver, and D. M. Neumark, J. Chem. Phys. **93**, 6108 (1990); C. C. Arnold and D. M. Neumark, *ibid.* **99**, 3353 (1993); C. C. Arnold and D. M. Neumark, *ibid.* **100**, 1797 (1994).
[7] E. C. Honea, A. Ogurn, C. A. Murray, K. Raghavachari, W. D. Sprenger, M. F. Jarrold, and W. L. Brown, Nature (London) **366**, 42 (1993).
[8] G. Burton, C. Xu, C. C. Arnold, and D. M. Neumark, Surf. Rev. Lett. (in press).
[9] K. Balasubramanian, J. Mol. Spectrosc. **123**, 228 (1987); Chem. Rev. **90**, 93 (1990).
[10] P. J. Bruna and F. Grein, Mol. Phys. **74**, 1133 (1991).
[11] G. Pacchioni, Mol. Phys. **49**, 727 (1983); Chem. Phys. Lett. **107**, 70 (1984).
[12] J. E. Kingcade, H. M. Nagarathna-Naik, I. Shim, and K. A. Gingerich, J. Phys. Chem. **90**, 2830 (1986).
[13] G. Herzberg, *Molecular Spectra and Molecular Structure*, Vol. 1, Spectra of Diatomic Molecules 2nd. ed. (Krieger, Malabar, 1989), p. 338.
[14] H. Lefebvre-Brion and R. W. Field, *Perturbations in the Spectra of Diatomic Molecules* (Academic, Orlando, 1986), pp. 100–109.
[15] R. J. Van Zee, R. F. Ferrante, and W. Weltner, Jr., J. Am. Chem. Soc. **83**, 6181 (1985).
[16] F. W. Froben and W. Schelze, Surf. Sci. **156**, 765 (1985).
[17] E. P. Wigner, Phys. Rev. **73**, 1002 (1948).
[18] L. M. Branscomb, D. S. Burch, S. J. Smith, and S. Geltman, Phys. Rev. **111**, 504 (1958); S. Geltman, *ibid.* **112**, 176 (1958).
[19] T. N. Kitsopoulos, I. M. Waller, J. G. Loeser, and D. M. Neumark, Chem. Phys. Lett. **159**, 300 (1989).
[20] T. G. Kietz, M. A. Duncan, D. E. Powers, and R. E. Smalley, J. Chem. Phys. **74**, 6511 (1981).
[21] D. Proch and T. Trickl, Rev. Sci. Instrum. **60**, 713 (1989).
[22] J. M. Bakker, J. Phys. E **6**, 785 (1973); **7**, 364 (1974).
[23] K. Müller-Dethlefs, M. Sander, and E. W. Schlag, Z. Naturforsch. Teil A **39**, 1089 (1984); Chem. Phys. Lett. **12**, 291 (1984); K. Müller-Dethlefs and E. W. Schlag, Annu. Rev. Phys. Chem. **42**, 109 (1991).
[24] J. Cooper and R. N. Zare, J. Chem. Phys. **48**, 942 (1968).
[25] J. B. Tatum and J. K. G. Watson, Can. J. Phys. **49**, 2693 (1971).
[26] K. F. Freed, J. Chem. Phys. **45**, 4214 (1966).
[27] A. E. Douglas, Can. J. Phys. **33**, 801 (1955); R. D. Verma and P. A. Warsop, *ibid.* **41**, 152 (1963).